

# An Experimental Study of Timber-Steel Hybrid Seismic Wall with tapered Joints

Ryo Sasaki<sup>1</sup>, Joichi Nakakuki<sup>2</sup>, Yuya Shirota<sup>3</sup>, Masamichi Sasatani<sup>4</sup>

**ABSTRACT:** The objective of this study is to develop a new timber-steel hybrid seismic wall system with timber panels inside a steel frame. This method uses tapered wedge joints at the four corners of the timber panel to integrate the steel frame and timber under bearing pressure and resists horizontal forces by the tensile force of steel and the compressive force of timber panels. The processes of bearing pressure installation is to tighten the wedge joints at the four corners. It doesn't need any requirement of clearance at various locations between timber and steel for the perspective of simplicity of construction. No-cracking due to long-term drying shrinkage because the timber is not constrained all the way around. To obtain basic data on the structural performance of this system, we conducted three different experiments in this study. Material experiments obtained the relationship between compression performance and fiber angle of timber. Wedge joint experiments confirmed that the joints follow the timber paxnel and the stress transfer paths. Shear wall experiments were conducted to study the structural performance as hybrid seismic walls, combining two types of timber panels (LVL and CLT) and two different aspect ratios.

**KEYWORDS:** Timber-Steel Hybrid seismic wall, Steel frame, Timber panel, Wedge joint

## 1 – INTRODUCTION

The purpose of this paper is to clarify the mechanical properties of a new hybrid structure combining timber and steel through experiments and to obtain basic data for practical application.

As a revised system different from the conventional system, we proposed a new timber-steel hybrid earthquake-resistant wall using tapered wedge joints with a pin mechanism (referred to as "wedge joint") shown as Figure1 and 2. The timber-steel hybrid earthquake-resistant wall (referred to as "hybrid seismic wall") consists of two timber panels, Laminated Veneer lumber (LVL) or Cross Laminated timber (CLT) panels, steel bar for prestressed braces (referred to as "PC steel rods") and wedge joints with a pin mechanism.

## 2 – BACKGROUND

There has been a noticeable move to promote the use of timber in Japan on the background of recent amendments to Japanese legislation. One result of this is an increasing number of examples of mid- and high-rise timber buildings. One of the construction methods is thought of

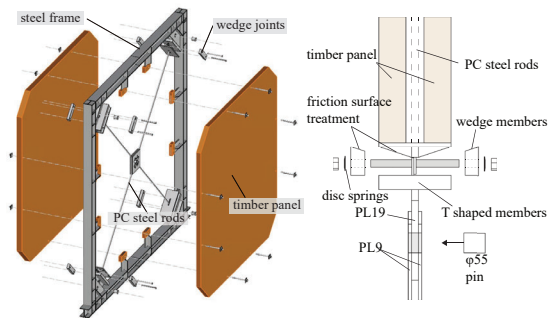


Figure1. Structural system overview

Figure2. Detail of joint

hybrid structures combining timber and steel. Using this hybrid construction concept, seismic wall system has been devised that incorporates timber panels in a steel frame to resist earthquakes [1][2]. The method of joining timber and steel for this system is generally integrated using drift pins or screws. The concern with this method is that cracking of the steel frame and timber panels may occur during and after construction due to drying shrinkage, resulting in reduced structural performance of the seismic wall. A hybrid seismic wall using wedge joints (referred to as the "conventional system") was

<sup>1</sup> Ryo Sasaki, Graduate School of Tokyo Denki university, Japan, 24fma31@ms.dendai.ac.jp

<sup>2</sup> Joichi Nakakuki, Former Graduate School of Tokyo Denki university, M.Eng, Japan, 22fma24@ms.dendai.ac.jp

<sup>3</sup> Yuya Shirota, Graduate School of Tokyo Denki university, Japan, 24fma32@ms.dendai.ac.jp

<sup>4</sup> Masamichi Sasatani, Prof, Tokyo Denki University, Dr. Eng, Japan, sasatani@mail.dendai.ac.jp

proposed as a joint type that solves the above problems [3]. The conventional system is to integrate timber panels and steel frames by wedge joints. However, this existing construction method left issues such as tracking performance during shear deformation, use of special cross-sections of timber panel or steel frames, and difficulty in panel fabrication.

### 3-STRUCTURAL SYSTEM OVERVIEW

#### 3.1 HYBRID SEISMIC WALL OVERVIEW

The load-bearing mechanism is shown in Figure 3. The characteristics of this hybrid seismic wall are compared with those of existing construction methods as below.

- (1) Long-term loads are supported by the steel frame, while horizontal loads are resisted by the two timber panels in compression. Tensile forces are carried by the PC steel rods to reduce stress loading of steel frames.
- (2) The joints used to integrate the timber panels and steel frames are tapered members that uses bolt tightening to create a state of support pressure. The joint between the steel frame and the wedge-shaped metalwork with a pin mechanism to ensure that all surface is in contact.
- (3) Since the timber panels and steel frames are supported by bearing pressure, A cracking against long-term shrinkage due to drying of the timber panels. This design also allows for the accommodation of construction tolerances and potential errors.
- (4) In the event of drying shrinkage after installation, the support surface is pushed up by the effect of the plate spring, which maintains the support with the timber panel.

(5) Timber panels are made lighter by using a pair of timber panels, so easy removal of timber panels is possible by loosening the steel bolts. This feature contributes to resilience and sustainability of buildings.

#### 3.2 OUTLINE OF COMPONENTS

This hybrid seismic wall system is designed for application in medium- to large-scale buildings and comprises the following components.

- (1) This system allows various timber panels to be used for seismic walls. In this study, LVL and CLT are adopted because of commonly distributed timbers and widely available for constructing of large-section face panels in Japan.
- (2) The steel frame accommodates a portion of the tensile force, which is balanced by the compressive capacity of the timber panels, thereby ensuring both seismic performance and long-term load-bearing capacity. The H-150 × 150 × 7 × 10 (SN490) cross-section was selected as the minimum size to ensure that the timber panels yield first.
- (3) The PC steel rods carry the tensile forces, which are balanced by the compressive forces of the timber panels. A φ17mm (SBPR 1080/1230) cross-section was selected as the minimum size to prevent yielding prior to the failure of the seismic wall. Joints that do not transmit compressive forces are placed in the centre and are connected to PC steel rods.
- (4) For the construction sequence, the wedge joints are pre-installed in the steel frame and the PC steel rod braces are installed. The timber panels are then placed on top and the wedge-shaped metal bolts are tightened to form a

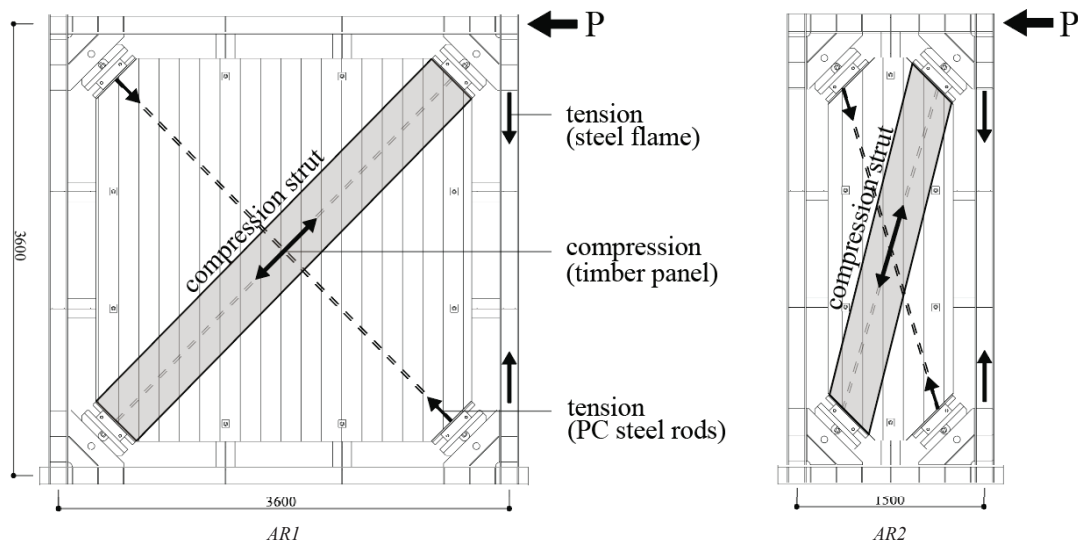


Figure3. Structural system for the earthquake

bearing pressure joint. The taper of the wedge joint was set to 1/3 slope, which has been confirmed to perform in conventional system [3]. Tapered surfaces were treated with a friction surface treatment using a rust accelerator.

## 4 – MATERIAL TEST

### 4.1 SPECIMENS AND SETUP

The test specimen variables are shown in Table 1, and the experimental setup is shown in Figure 4. The performance of the hybrid seismic wall is derived from the formation of compression struts within the timber panels. Therefore, compression tests were conducted at various angles for LVL and CLT to obtain the relationship between the fiber orientation of the timber panels and their characteristic properties. Considering the aspect ratios of the 3600 mm and 1500 mm spans as Figure 3 used in this seismic wall, the experimental variables for the 3600 mm span model (hereafter referred to as S-AR1) included angles of 0, 30, 45, 60, and 90 degrees between the direction of applied force and the fiber orientation. For the 1500 mm span model (hereafter referred to as S-AR2), the experimental variables included angles of 0, 14, and 90 degrees. The LVL specimens measured  $75 \times 75 \times 150$  mm, while the CLT specimens measured  $90 \times 90 \times 180$  mm. Three specimens were used for each LVL and six for each CLT, based on the characteristics of the lumber. Simple compressive loading carried out over approximately 5 minutes until failure occurred by a universal compression testing machine (capacity: 1000 kN) [4].

### 4.2 RESULT

The results of the experiment are presented in Figure 5. The following findings were observed from the experiment.

Failure of the LVL specimens occurred due to fiber buckling at 0 degree, cracking along the fiber direction at 14, 30, and 45 degrees, and veneer buckling at 60 and 90 degrees. The compressive strength generally followed a hyperbolic relationship at 14 and 30 degrees, and aligned with the Hankinson equation at 45 and 60 degrees. Additionally, Young's modulus was found to generally correspond with the Hankinson equation across all angles.

Failure of the CLT specimens occurred due to fiber buckling at 0 degree, cracking at the lamina width-breaking position at 14, 30, 45, and 60 degrees, and buckling of the fibers in the orthogonal layer lamina at 90 degrees. The compressive strength of each lamina generally followed the curve predicted by the equivalent section method using the Hankinson equation. However, the strength of specimens exhibiting cracks at the solid

Table 1. specimens of material test

		$\theta(^{\circ})$					
		0	14	30	45	60	90
S-AR1	LVL	3	-	3	3	3	3
	CLT	6	-	6	6	6	6
S-AR2	LVL	3	3	-	-	-	3
	CLT	6	6	-	-	-	0

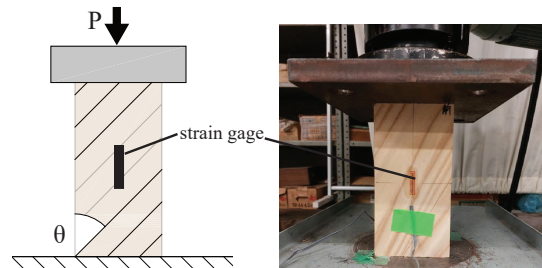


Figure 4. setup of material test

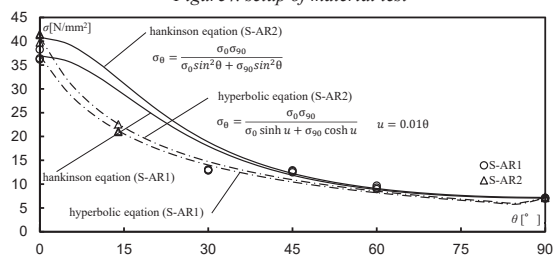


Figure 5(a). compressive strength of LVL

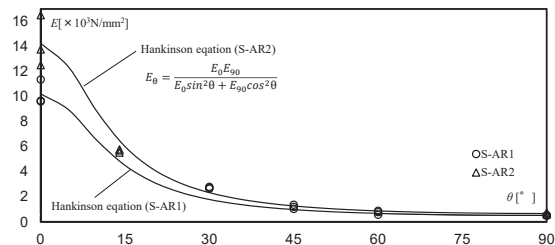


Figure 5(b). Young's modulus of LVL

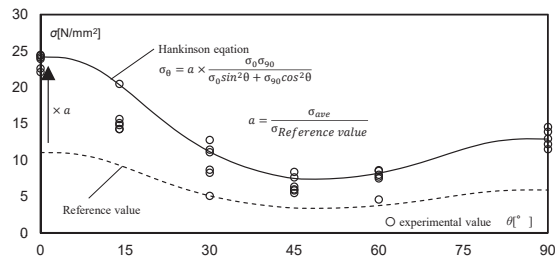


Figure 5(c). compressive strength of CLT

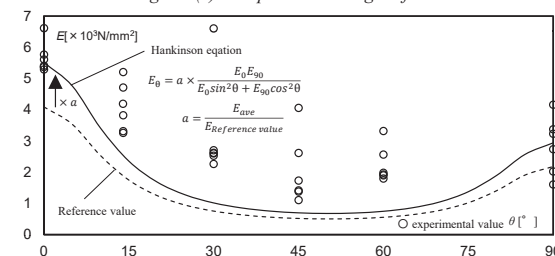


Figure 5(d). Young's modulus of CLT

laminated position was significantly lower, particularly at 14 and 30 degrees, highlighting a marked difference in fracture properties. Young's modulus for each lamina was also compared with the Hankinson curve, and the two sets of values generally showed good relationship. However, the calculated values varied significantly depending on the position of the lamina. In all cases, the calculated values were higher than those predicted by the Hankinson curve, regardless of the angle.

## 5 – JOINT TEST

### 5.1 SPECIMENS AND SETUP

Details of the wedge joint and experimental set-up are shown in Fig. 6. The experiment confirmed that the wedge joints did not separate as the timber dried and shrank, that the support surfaces conformed to the timber panels, and that the joints transferred stresses as anticipated.

Test specimens are steel and full-size wedge joints. The forces were applied using a compression testing machine (capacity 2000 kN) according to the following procedure.

- (1) Tighten the bolts of the wedge members by hand to establish the contact condition.
- (2) Load the joints with 30 kN using the compression testing machine.
- (3) Tighten the bolts and disc springs of the tapered members using a torque wrench to apply a force of 30 Nm.
- (4) Unloading at a constant speed.

### 5.2 RESULT

The behaviour of the tapered member is shown in Figure 7. When the wedge-shaped metalwork has moved by 0.49 mm, the supporting surface has moved by 0.15 mm. The results show that the ratio of the displacement is approximately 3:1, which is same with the taper angle of the wedge-shaped metal and confirms that the pressure surface is followed by the disc spring. The minimum principal stress directions measured by triaxial strain gauges confirm that the stresses are transferred as expected to the frame via the pin connection.

## 6 – SHEAR WALL TEST

### 6.1 SPECIMENS AND SETUP

The shape of the test specimen is shown in Figure 8, the experimental setup in Figure 9, and the test procedure in Figure 10. The mechanical properties of the timber panels

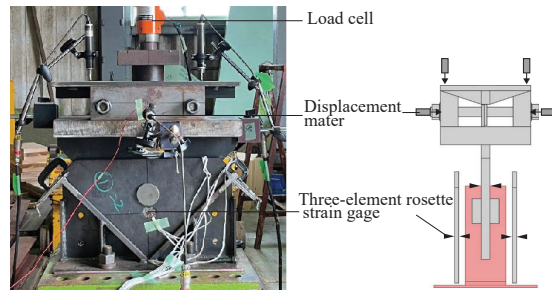


Figure 6. Joint test specimen and setup

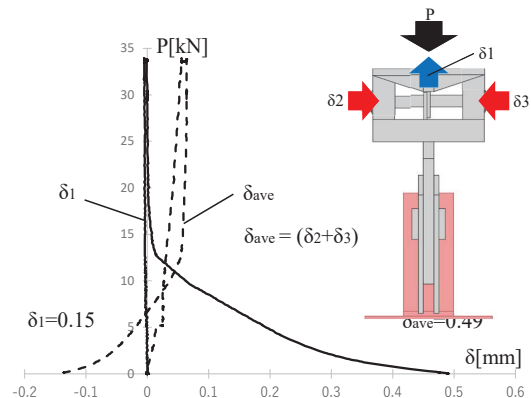


Figure 7. Joint test load-deformation curve

were determined through material testing as session 4, and a total of four test specimens were carried out. The experimental parameters were column span and wood panel type.

The specimens were single-layer, single-span at full scale, with a beam core distance of 3600 mm. Two column span lengths were 3600 mm (referred to as AR1) and 1500 mm (referred to as AR2). The steel frame cross-section consisted of H-150 × 150 × 7 × 10 (SN490) and was reinforced with stiffeners at appropriate locations, especially at the four corners to form pin joints. The LVL panels were constructed from 75 mm thick, 3050 mm high, 3000 mm wide, E70-1 grade (40V-34H) cedar timber, with a moisture content of less than 20%. The CLT panels were made of 90 mm thick, 3050 mm high, 3000 mm wide, S60 grade (3-ply, 3-layer) cedar timber, also with a moisture content of less than 20%. The steel frame was constructed from H-steel, secured to the reaction frame along its entire length using high-strength bolts. In AR1, four PC steel rods with a diameter of  $\phi 17$  mm and a length of 2020 mm were used, while in AR2, four PC steel rods with a diameter of  $\phi 17$  mm and a length of 1455 mm were adopted. Eight buckling stoppers were installed in AR1 and six in AR2.

The experimental method and measurement points are shown in Figure 9. Compressive forces were applied from both sides using hydraulic jacks (capacity: 1000 kN,

200 mm), which were installed at the center of the upper beam of the steel frame. The inter-story deformation angles,  $R = 1/450, 1/300, 1/200, 1/150, 1/100, 1/75,$  and  $1/50,$  were applied in alternating positive and negative directions, with each angle repeated three times.

The load was then applied simply on the positive force side until either the stroke limit was reached or a 20% reduction in load from the maximum load occurred. Measurements included the horizontal deformation of the steel frame, displacement of the column legs, and relative deformation between the timber panel and steel frame. Axial strain in the columns and PC steel rods, as well as the principal stress direction in the timber panels, were measured using uniaxial and triaxial strain gauges, respectively.

## 6.2 RESULT

### (1) Fracture properties

The experimental results are shown in Table 2, and the key fracture properties are shown in Figure 11. The two primary fracture modes observed were cracking along the fiber direction of the timber panel and penetration of the timber panel into the joint support surface.

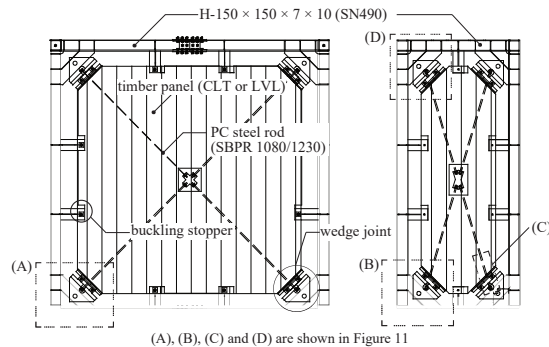
<Model with the LVL panel inserted in AR1 (AR1-1)>

A distinct sound was emitted from the timber panel early in the load application process in AR1-1, although no visible damage was observed at  $R = 1/450.$  At  $R = 1/50,$  the timber panels were found to be significantly embedded into the joint support surface. The LVL panel deformed out-plane, and the surface layer of the panel cracked and delaminated near the bearing surface. In the steel frame, the bottom flange of the foundation H-steel yielded and deformed into a rippled shape. Cracking near the bearing surface progressed at  $R = 1/32,$  and the LVL panel was found cracking along the fiber direction, leading to a reduction in load capacity.

<Model with the CLT panel inserted in AR1 (AR1-2)>

In AR1-2, the sound of the CLT panel of the wall was noticeable from the early stages. After  $R = 1/300,$  the sound of the CLT panel of the wall continued. In-plane rotational behavior similar to AR1-1 was observed. At  $R = 1/100,$  metallic noise was heard near the wedge joints, and at  $R = 1/75,$  the holes in the gusset plate that received the pin connection of the joints began to deform, as if being pushed apart by the compression force from the CLT panel. At  $R = 1/50,$  the CLT panel was found to be embedded in the surface of the wedge joint, and sliding CLT panel became more pronounced, while further

deformation of the wedge joint and embedding progressed. The joint deformed around  $R = 1/60$  during the first cycle of the negative force at  $R = 1/50,$  and the CLT panel exhibited noticeable deformation, leading to a decrease in load.



(A), (B), (C) and (D) are shown in Figure 11

Figure 8. Shear wall test specimen

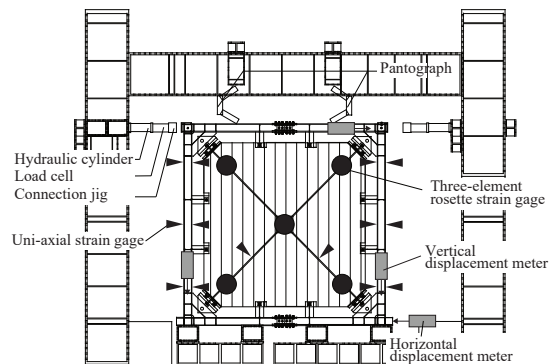


Figure 9. Shear wall test setup



Figure 10. Shear wall test process

<Model with the LVL panel inserted in AR2 (AR2-1)>

In AR2-1, similar to the AR1 series, the LVL panel initially produced a cracking sound and exhibited in-plane rotation at  $R = 1/200.$  Due to this rotation, the LVL panel did not maintain uniform contact with the support surface of wedge joint. At  $R = 1 / 150,$  sliding behavior

of the PC steel rod's nut was observed as the deformation angle progressed, and at  $R = 1 / 100$ , the LVL panel was found to be dented around the corner. After  $R = 1/75$ , the load fluctuated repeatedly as the threads at the end of the PC steel rods contacted with the wedge joint and the applied force was continued. The experiment was ultimately terminated after the force was applied up to the stroke limit at  $R = 1/19$ , as no substantial failure occurred.

<Model with the CLT panel inserted in AR2 (AR2-2)>

AR2-2 exhibited similar behaviour to AR2-1 up to a displacement ratio of  $R = 1/200$ . However, at  $R = 1/150$ , it was observed that the CLT panel was found to be dented around the support surface of wedge joint. The test was subsequently terminated after the force was applied up to the stroke limit of  $R = 1/17$ .

(2) Historical properties

Dimensionless hysteresis curves at  $R = 1/300$ ,  $1/200$ , and  $1/50$  are shown in Figure 12, while the historical properties of each specimen are shown in Figure 13. These dimensionless hysteresis curves were derived by normalizing the third cycle of each deformation angle with respect to the maximum load and displacement.

<AR1-1> Stiffness began to decrease at  $R = 1/100$ , and out-plane deformation of the panel was found after  $R = 1/50$ , leading to a gradual reduction in stiffness. At  $R = 1/50$ , the maximum load ( $P_{max}$ ) in the first cycle on the positive side was 848 kN, and the deformation remained relatively constant under load until failure occurred during the push-off phase.

<AR1-2> Similar to AR1-1, stiffness began to decrease at  $R = 1/100$ . The load dropped sharply due to flexural yielding of the joints and the CLT panels during the first cycle on the negative side at  $R = 1/50$ , which led to failure during the first cycle on the negative side at  $R = 1/60$ . Compared to AR1-1, the yield capacity, initial stiffness, and maximum load capacity increased by factors of 1.37, 1.18, and 1.05, respectively, but ductility factor became 0.69.

<AR2-1> Stiffness began to decrease at  $R = 1/100$ . During the first cycle on the positive side at  $R = 1/75$ , the load decreased by approximately 80 kN due to contact between the PC steel rods and the joint. However no significant failure occurred, and stiffness remained unaffected. After  $R = 1/50$ , the load continued to increase slightly with deformation progressing up to the stroke limit.

<AR2-2> The stiffness did not decrease significantly until  $R = 1/50$ . After  $R = 1/50$ , the load continued to

Table2. Shear wall test characteristic value

	Yield strength [kN]	Yield displacement [mm]	initial stiffness [kN/mm]	ultimate strength [kN]	ultimate displacement [mm]	maximum capacity [kN]	
AR1	-1	470	36.0	13.0	776	110.1	848
	-2	644	42.1	15.3	853	71.6	893
AR2	-1	242	58.4	4.1	356	85.9	392
	-2	286	69.9	4.1	362	88.3	397



Figure11. Fracture properties

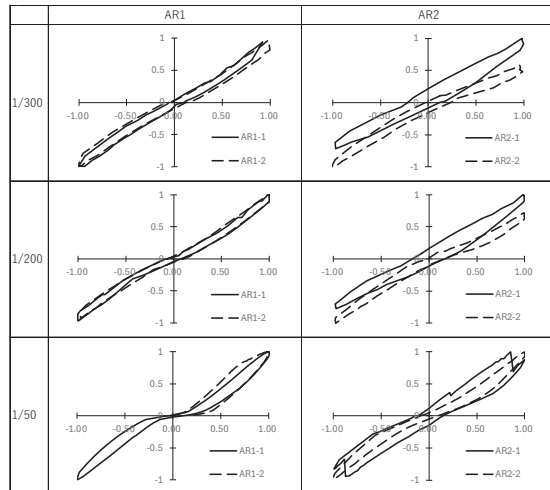


Figure12. dimensionless hysteresis curve

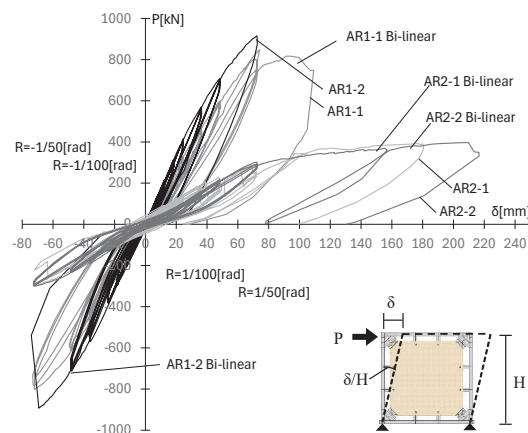


Figure13. Shear wall test load-deformation curve

increase slightly as the CLT panel became embedded and deformed up to the stroke limit. The characteristic values and the shape of the history curves indicate that the AR2 series exhibits stability better compared to the AR1 series, suggesting more dominant influence of the steel frame.

### (3) Effect of timber panel type and aspect ratio

Both AR1-1 and AR1-2 showed elastic historical properties. Especially in the historical area, AR1-2 had high energy absorption capacity at all deformation angles. It is suggested due to the difference in energy absorption capacity of CLT composed of three layers of lamina, compared to LVL composed of veneers.

In the AR2 series, in-plane rotation was observed due to the aspect ratio of the timber panel. The positive and negative historical properties are different at small deformation angles, and Positive and negative deformations showed similar characteristics up to around  $R=1/50$ . Same as AR1 series, AR2-2 with CLT panels shows larger historical area at  $R=1/50$ .

The yield and maximum bearing capacity of the AR1 series was approximately twice that of the AR2 series, and initial stiffness was more than triple. It is suggested that AR1 with aspect ratio of 1 allows for a larger compression strut width than AR2 and efficiently resisted horizontal forces by timber panels. The ductility factors were 0.61 for AR1-1 and 0.56 for AR2-1. It is suggested that AR1 is smaller aspect ratio than AR2 and timber panel shape were effective in shear resistance.

### (4) Shear force burden ratio

The axial force and bending moment curve are shown in Figure 14, and the envelope of each borne shear force for the timber panel and the steel frame with PC steel rods bracing is shown in Figure 15.

From the correlation chart between axial force and bending moment, it is suggested that both AR1 and AR2 series intersected with the yield line around  $R=1/100$  so that it reduced in stiffness of the seismic wall, and the steel columns yielded. AR1-2, which has a larger column axial force than AR1-1 with LVL, shows a larger ratio of axial force borne to bending moment. AR2 series were a larger ratio of bending moment borne to axial force than AR1 series.

The axial force  $N_s$ , bending moment  $M_s$ , shear force  $Q_s$ , and borne shear force  $Q_{pc}$  of the PC steel rods were obtained from the axial strains of the steel columns and PC steel rods, and the difference between the shear force  $Q$ ,  $Q_s$ , and  $Q_{pc}$  acting on the entire test piece was used as

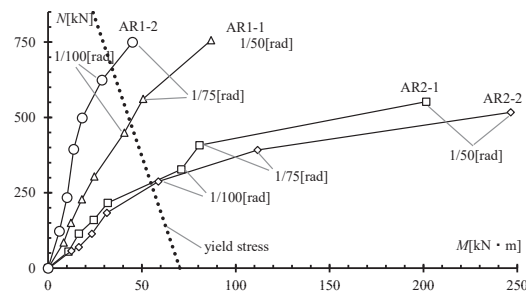


Figure 14. Axial Force - Bending Moment curve

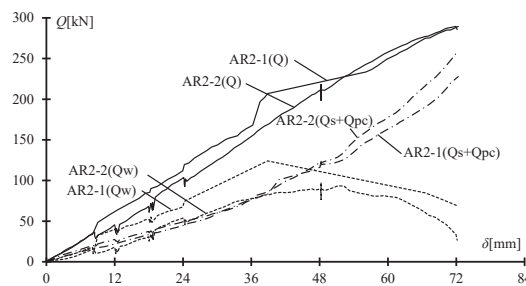


Figure 15(a). Shear Force Contribution Ratio (AR1 Series)

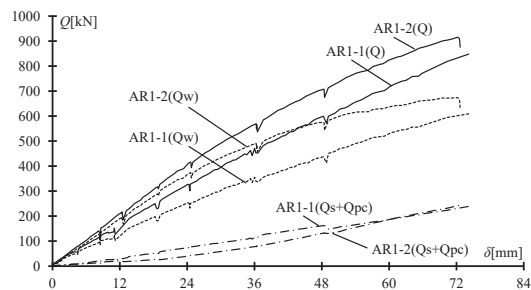


Figure 15(b). Shear Force Contribution Ratio (AR2 Series)

the borne shear force  $Q_w$  of each timber panel. The calculation formula is shown below.

$$N_s = \varepsilon_{ave} \times E \times A = \{(\varepsilon_i + \varepsilon_{i+1})/2\} \times E \times A \quad (1)$$

$$M_s = \varepsilon_{def} \times E \times Z = \{(\varepsilon_i - \varepsilon_{i+1})/2\} \times E \times Z \quad (2)$$

$$Q_s = (M_t + M_b) / L \quad (3)$$

$$Q_{pc} = \varepsilon_{pc} \times E_{pc} \times A_{pc} \times \cos \theta \quad (4)$$

$$Q_w = Q - (Q_s + Q_{pc}) \quad (5)$$

Here,  $M_t$  the top column bending moment,  $M_b$  the bottom column bending moment,  $\theta$  the angle between the PC steel rods and the steel beam, and  $L$  the distance over which strain is measured.

In the elastic range as  $R=1/200$ , the ratio of shear force on the timber panel to that on the steel frame was 4:1 for AR1-1 and 10:1 for AR1-2. The AR2 series was 1:1, and the steel frame was more dominant than the AR1 series.

## 7– CONCLUSION

In this study, various experiments were conducted to confirm the structural performance of a new timber-steel hybrid seismic wall system with timber panels inside a steel frame. As a result, basic data contributing to the design of this seismic wall were obtained as below.

- The new system of hybrid seismic wall proposed five improvements from the existing system
- Based on material tests with LVL and CLT, the relationship between the angle of compressive force and the strength and stiffness in the fiber direction was obtained from the Hankinson Curve.
- Structural performance of wedge joints was obtained from compression tests of the joints at the four corners.
- The structural behavior and stiffness of the hybrid seismic wall were obtained from horizontal tests of aspect ratio (AR1 or AR2) and timber material (LVL or CLT).

## 8 – ACKNOWLEDGEMENT

This work was partially supported by Research Institute for Science and Technology of Tokyo Denki University Grant Number Q22T-02/Japan.

## 9 – REFERENCES

- [1] K. Fukumoto “A case study and future subjects of steel frame hybrid structure with CLT infill shear walls” *AIJ J. Technol. Des.* Vol. 26, No.64, 923-928, Oct, 2020.
- [2] H. Shiote “Development of hybrid Seismic System with steel Frame and LVL Part1 An overview of the system, case studies” *AIJ, Hokuriku, Chapter Architectural Research meeting*, pp129-130, September 2010.
- [3] M. Sasatani “The development of hybrid shear wall with stuck laminated panel and steel frame” *AIJ J. Technol. Des.* Vol. 21, No.49, 1037-1042, Oct, 2015.
- [4] Architectural Institute of Japan, *Kenchiku zairyo jikkenn - yo kyoza*i [Architectural materials experimental textbook]. Architectural Institute of Japan, March 2000, pp. 75-76.